

OPEN

Retina Publish Ahead of Print

DOI: 10.1097/IAE.0000000000003928

## Retinal Tectonics after Macular Pucker Surgery: Thickness Changes and En-Face Displacement Recovery

Fabio Scarinci MD\*, Giorgio Querzoli PhD\*\*, Pamela Cosimi MD\*, Guido Ripandelli MD\*, Mario R. Romano MD, PhD<sup>^</sup>, Andrea Cacciamani MD\*, Marion R. Munk MD<sup>^^</sup>, Tommaso Rossi MD\*

\* IRCCS Fondazione Bietti ONLUS – Roma, Italy

\*\* DICAAR – Università di Cagliari, Italy

<sup>^</sup> Department of Biomedical Science, Humanitas University, Milan, Italy

<sup>^^</sup> Augenarzt-Praxisgemeinschaft Gutblick AG, Pfäffikon, Switzerland

Feinberg School of Medicine, Northwestern University, Chicago, IL

Inselspital, University Hospital Bern, Bern, Switzerland · Department of

Ophthalmology

This is an open-access article distributed under the terms of the Creative Commons Attribution-Non Commercial-No Derivatives License 4.0 (CCBY-NC-ND), where it is permissible to download and share the work provided it is properly cited. The work cannot be changed in any way or used commercially without permission from the journal.

Copyright © 2023 The Author(s). Published by Wolters Kluwer Health, Inc. on behalf of the Ophthalmic Communications Society, Inc.

Running Title: Enface Retinal Displacement after pucker

Financial disclosure: None of the authors has any competing or conflict of interest related to the subject matter.

Acknowledgements: The Authors would like to thank the “Fondazione Roma” and the Italian Ministry of Health for financial support. The Authors would also like to thank Giuliana Facciolo and Francesca Petruzzella for patient study and image analysis.

Corresponding author:

Tommaso Rossi MD

IRCCS Fondazione Bietti ONLUS - Via Livenza 3, 00198 Roma

e-mail: [tommaso.rossi@usa.net](mailto:tommaso.rossi@usa.net) - tel +39 348 2645034

Word count: XXX

## Summary

The removal of epiretinal membranes determines thickness changes in all retinal layers causing the re-distribution of forces of the entire retinal architecture and marked tangential displacement. Both thickness changes and *en-face* deformation correlated with visual function.

## Abstract

**Purpose:** To study visual function, retinal layer thickness changes and tangential displacement after Pars Plana Vitrectomy (PPV) for EpiRetinal Membrane (ERM).

**Methods:** Retrospective series of patients undergoing PPV for ERM, with 6-month follow-up including best-corrected visual acuity (BCVA), Optical Coherence Tomography (OCT), M-charts, ERM grading, and InfraRed fundus photo at time 0 (T0, pre-op) at month 1 (T1), 3 (T3), 6 (T6) post-op ( $\pm 1$  week). Retinal layer thickness and tangential (*en-face*) retinal displacement between successive times for the entire retinal surface and the central horizontal and vertical meridian were also measured. *En-face* displacement was calculated as optical flow of consecutive images.

**Results:** Average BCVA improved from  $0.28 \pm 0.08$  logMAR at T0 to  $0.16 \pm 0.25$  at T6 ( $p=0.05$ ), BCVA improvement correlated with BVCA at T0 ( $p<0.001$ ). Vertical metamorphopsia decreased from  $1.33^\circ \pm 0.70^\circ$  at T0 to  $0.82^\circ \pm 0.69^\circ$  at T6 ( $p<0.05$ ). Foveal thickness reduced from  $453 \pm 53 \mu\text{m}$  at T0 to  $359 \pm 31 \mu\text{m}$  at T6 ( $p<0.05$ ) and reduction correlated with BCVA improvement ( $p<0.05$ ). Foveal layers decreased ( $p<0.05$ ) in all cases. Mean *en-face* deformation was  $155.82 \pm 50.17 \mu\text{m}$  and mostly occurred in the first month: T0-T1 displacement was  $83.59 \pm 30.28 \mu\text{m}$ , T1-T3 was  $36.28 \pm 14.45 \mu\text{m}$ , while T3-T6 was  $39.11 \pm 22.79 \mu\text{m}$  ( $p<0.001$ ) on average. Peri-foveal and parafoveal deformation correlated with OCT foveal thickness reduction at all time intervals (1, 3, 6 months:

p<0.01).

**Conclusion:** ERM peeling affects all retinal layer thickness and results in new force balance across the entire retina and tangential displacement. Both *en-face* and in-depth changes correlate with visual function.

**Keywords:** Metamorphopsia; Epiretinal Membrane, Macular Pucker; Retinal Layer

## Introduction

Idiopathic Macular Pucker is a pathologic condition due to the anomalous or incomplete posterior vitreous detachment leaving posterior hyaloid remnants adherent to the retinal surface<sup>1</sup>, more accurately referred to as idiopathic EpiRetinal Membranes (ERMs). The subsequent contraction of adherent vitreous may exert tangential traction over the inner and outer retina, causing irregular retinal displacement, macular thickening, and visual disturbance<sup>2</sup>.

Metamorphopsia defined as the deformation of visual perception<sup>3</sup> and the deterioration of visual acuity are the functional hallmarks of symptomatic ERMs and may impact on patients' quality of life<sup>4</sup> prompting surgical removal.

Metamorphopsia has been ascribed to the degree of retinal layer disorganization and the misalignment of retinal layers causing Muller cells bending in EMRs<sup>5 6</sup>, diabetic macular oedema<sup>7</sup> and retinal vein occlusion<sup>8</sup>; however, the precise attribution of visual symptoms to anatomic changes remains elusive.

Pars Plana Vitrectomy (PPV) with ERM peeling may reduce the retinal deformation, decrease metamorphopsia and improve visual acuity<sup>9</sup>. The mechanism underlying the reduction of metamorphopsia, and the recovery of vision has not yet been fully elucidated; however, it has been associated to cellular function recovery and microarchitectural changes<sup>10</sup>.

Purpose of present study is to evaluate retinal layers thickness changes and in-plane (“en-face”) displacement after PPV and their association with visual function: visual acuity and metamorphopsia.

## Materials and Methods

### Study participants

We retrospectively analysed all patients undergoing PPV and peeling for idiopathic ERM affecting the fovea classified as stage 2-3 according to Govetto<sup>11 12</sup> with a disease duration <3 years. All patients received surgery at the IRCCS Bietti Foundation between January and June 2022 and had been operated by a single surgeon. Diagnosis was confirmed by ophthalmoscopic examination and Spectral Domain Optical Coherence Tomography (SD-OCT). The study was conducted at the Ophthalmology Department of the Bietti Foundation between January and November 2022.

Exclusion criteria were as follows: 1) history of ocular and specifically macular disorders including age-related macular degeneration, retinal vascular occlusions, retinal detachment, trauma, high myopia (ocular axial length >26.00 mm), and uveitis; 2) history of systemic diseases, including hypertension and diabetes; 3) poor imaging quality due to media opacity; 4) incomplete chart or records.

Seventeen patients (10 females and 7 males) met inclusion criteria and received complete ophthalmologic assessment, patent and manifest refraction, Best Corrected Visual Acuity (BCVA) using Early Treatment Diabetic Retinopathy Study (ETDRS) acuity charts and Snellen visual acuity converted to the logarithm of Minimum Angle of Resolution (logMAR) units for statistical purposes and indirect ophthalmoscopy. The degree of horizontal and vertical metamorphopsia was assessed via M-CHARTS (Inami, Co, Tokyo, JAPAN)<sup>13</sup>; retinal sensitivity was obtained with microperimetry, and SD-OCT

scan was also performed. All included patients had the above information available at time 0 (pre-op), time 1, 3, 6 months ( $\pm 7$  days) after surgery.

All patients provided written informed consent, the study adhered to the tenets of the Declaration of Helsinki and received approval of the local Ethics Committee (ERMLAB01 N° 77/18/FB).

### Surgical procedure

All patients underwent a standard 25-gauge 3-port PPV with ERM and Internal Limiting Membrane (ILM) peeling with single Brilliant Blue G staining (Kemin Pharmaceutica Unipessoal, LTDA, Des Moines, IA).

### Optical coherence tomography image acquisition

Spectral domain OCT (Spectralis HRA-OCT, version 1.5.12.0; Heidelberg Engineering, Heidelberg, Germany) images were acquired using the horizontal SD-OCT cross-section (an average of 25-30 frames for each B-scan was used to improve image quality as elsewhere reported<sup>14</sup>). Baseline acquisitions were taken before surgery (T0) and repeated with follow-up function was set at 1 month (T1), 3 months (T3) and 6 months (T6) post-surgery. Prior to data assessment, the extract centration and location of the OCT scan was checked and if needed manually corrected. The segmentation of the retina was obtained using automatic built-in software and all SD-OCT scans were segmented into four layers as described in<sup>15</sup>. Due to the pathologic changes induced by the ERM itself, the inner retinal layers appeared at times indistinguishable in OCT images. For this reason, we cumulatively defined as "Inner Retina" (IR), the most inner layer comprising the internal limiting membrane the retinal nerve fiber layer (ILM+RNFL), the ganglion cell layer (GCL) and inner plexiform layer (IPL) (IRL=ILM+RNFL+GCL+IPL). The central 1mm foveal

thickness, inner nuclear layer (INL), outer plexiform layer (OPL), and outer nuclear layer (ONL) remained always distinguishable in OCT and were therefore analysed as such.

Retinal layer thickness considered in the analysis were also divided by EDTRS sectors: foveal central 1mm, superior, temporal, inferior and nasal. Concentric circles indicated the foveolar region (radius 0.5 mm), perifoveal (radius 1.5 mm) and parafoveal (radius 3 mm).

### Measurements of the retinal en-face deformation

*En-face* dislocation was measured by comparing couples of successive images taken at baseline and (month 0), and after 1, 3, and 6 months. Thus, we present and discuss the deformation during the first month after surgery (T0-T1), the successive two months (T1-T3) and the additional 3 months (T3-T6). Displacements between consecutive images were computed on a regular grid (36×36 nodes) using the Farneback two-frame motion estimation method<sup>16</sup> which is based on the idea of comparing the neighbourhoods of corresponding nodes on the two images to find the translation between them. Preliminarily, the grey levels of the images were inverted and pre-processed to obtain a uniform enhancement of the details over the single image and between images. Small image portions were independently analysed, and the contrast was locally modified to obtain a uniformly flat intensity histogram. Then, each couple of images was corrected for a rigid roto-translation to discard the differences due to the different orientation and centration of the two analyses and thus obtain two perfectly aligned images. At that aim i) the map of the two-component displacements was computed by the Farneback algorithm; ii) the roto-translation minimizing the Sum of the Square Differences (SSD) of the 36×36 calculated displacements was found; iii) the roto-translation was applied to the second image to subtract the misalignment between them; iv) the above procedure (consisting of steps ii and iii) was iterated until convergence (*i.e.* when SSD varied less than 3% between two

consecutive iterations). After the roto-translation removal, the retinal deformation was obtained on the same grid by using again the displacement detection algorithm. The small marginal non-overlapping regions at the borders of the images were excluded from the latter step.

We analysed the results (shown as vector fields) both over the whole image and in the regions of interest shown in figure 1: the circular region 0.5mm in radius, (hereafter referred to as “central”); two circular crowns with the same centre and radius ranging from 0.5 mm to 1.5 mm (“perifoveal”) and from 1.5 up to 3mm (“parafoveal”); the 1 mm wide region adjacent to a horizontal and a vertical line crossing on the foveola (horizontal and vertical meridian, respectively). In order to let the reader visually perceive the changes, in figure 1, as well in the following figures, we superimposed the two analysed images using pseudo-colours: the first image is red, while the second is green. Thus, red represents details that were present only in the first image while green represents details present only in the second image. Details present in both images (indicating that no changes occurred during the considered time) results yellow (i.e. red+green).

The two components ( $D_x$ , horizontal and  $D_y$ , vertical) of the displacement are obtained in microns and the statistics such as mean values are computed using the displacement magnitude of the vectors  $D = \sqrt{D_x^2 + D_y^2}$  included in the region of interest (the whole image or one of the above mentioned).

### Main Outcome Measures

Main study outcome measures included BCVA, M-Charts Grading, microperimetric retinal sensitivity, retinal layers thickness, overall foveal thickness, mean *en face* displacement and the correlation between functional and anatomic changes.



## Statistical Analysis

The Analysis of Variance (ANOVA) with t-test and t-test for repeated measures applied to numerical variables were used to assess changes at different time-points. Bivariate Pearson's r correlation coefficient was applied for continuous variables, while Spearman's rho and Kendall's Tau were used for the assessment of ordinal variables such as ERM classification grades. Shapiro-Wilk test was employed for the Gaussian distribution of data.

In all cases p values < 0.05 were considered statistically significant.

## **Results**

### Visual acuity and metamorphopsia

Sample population included 17 patients (7 males and 10 females); mean age was  $74.8 \pm 7.9$  years with no significant difference between sexes. Average BCVA significantly improved from  $0.28 \pm 0.08$  logMAR at T0 to  $0.16 \pm 0.25$  at T6 months (0.49 to 0.68 Snellen;  $p < 0.05$ ) and BCVA improvement correlated to BVCA at T0 ( $p < 0.001$ ; table 1).

Horizontal metamorphopsia did not change significantly ( $0.91^\circ \pm 0.70^\circ$  at T0 Vs  $0.78^\circ \pm 0.56^\circ$  at 6 months; n.s.), while vertical metamorphopsia decreased during the study follow-up ( $1.33^\circ \pm 0.70^\circ$  at T0 versus  $0.82^\circ \pm 0.69^\circ$  at T6;  $p < 0.05$ ).

### Retinal layer thickness changes

The overall foveal thickness reduced from  $453 \pm 53$  at T0 to  $359 \pm 31$  microns at T6 months and the amount of thickness reduction correlated with BCVA improvement ( $p < 0.05$ ). Most of the foveal thinning was due to the Inner Retinal Layer thickness reduction which significantly decreased in each considered ETDRS sector ( $p < 0.05$  in all cases; fig. 2). Thickness reduction correlated with ERM grading ( $p < 0.016$ ).

All other deeper retinal layers showed only sectorial significant thinning reported in figure 3: the INL and OPL of the central foveolar, superior, and temporal subfield sectors reduced their thickness at the INL and OPL thickness decreased ( $p < 0.05$ ) while only the ONL thickness of the central foveolar subfield significantly decreased during the study ( $p < 0.05$ ; fig. 3).

### Retinal en-face displacement

*En-face* displacement magnitude, averaged over the entire central field and the 6-months follow-up was  $155.82 \pm 50.17 \mu\text{m}$ . Displacement mostly occurred during the first month post-surgery: mean displacement was  $83.59 \pm 30.28 \mu\text{m}$  between T0-T1 vs  $36.28 \pm 14.45 \mu\text{m}$  between T1-T3 ( $p < 0.001$ ) and  $39.11 \pm 22.79 \mu\text{m}$  between T3-T6 (not significant; Table 2). All considered concentric regions underwent a significantly higher displacement within the first month ( $p < 0.05$  for all) and displacement increased with eccentricity, as the annular ring with radius ranging from 1.5 mm to 3 mm suffered a higher average displacement compared to the fovea in the first 3 months (table 2;  $p < 0.01$  in all cases).

The *en-face* deformation along the “central cross” was  $36 \pm 13 \mu\text{m}$  across the horizontal and  $41 \pm 14 \mu\text{m}$  across the vertical meridian, the difference being not statistically significant.

Peri- and para-foveal deformation correlated with SD-OCT foveal thickness reduction at all time intervals (T0-T1, T1-T3, T3-T6;  $p < 0.01$  for all). Both overall foveal and IRL thinning strongly correlated with the *en-face* displacement ( $p < 0.01$  for both).

*En-face* displacement did not correlate with BCVA or microperimetric retinal sensitivity. The displacement along the vertical line correlated with the improvement in horizontal metamorphopsia ( $p < 0.028$ ). The distribution of *en-face* displacement compared

to visual acuity changes, followed a Gaussian normal distribution ( $p < 0.05$ ; fig. 4). *En-face* displacement also correlated with deeper layers thickness decrease such as INL central ( $p = 0.007$ ), INL perifoveal nasal ( $p = 0.011$ ), ONL central ( $p = 0.012$ ).

Epiretinal membranes classification correlated with the overall tangential deformation ( $p = 0.019$ ), vertical and horizontal retinal deformation ( $p < 0.01$  for both).

BCVA at T0 correlated with the perifoveal ( $p = 0.036$ ) and parafoveal ( $p = 0.04$ ) *en-face* deformation in T3-T6. M-Charts scoring change between any given time-point does not correlate either with BCVA improvement, retinal thickness changes or *en-face* retinal deformation over the whole investigation region.

## Discussion

Pars plana vitrectomy with ERM peeling can stop disease progression and improve vision and metamorphopsia;<sup>17</sup> however, the underlying ultrastructural mechanisms remain poorly understood<sup>18</sup>.

Our data confirm that ERM is a full-thickness disease and peeling impacts the whole retina, affecting both inner and outer layers (fig. 3); likewise, the degree of retinal disruption graded by the ERM classification<sup>13</sup> correlated with *en-face* displacement and post-operative thickness reduction at all levels.

Peeling manoeuvres released the internal tensions of the tissue thus modifying the post-operative retinal structure three-dimensionally, a process more pronounced in the first 30 days but spanning over the entire 6-months of follow-up time (fig. 5). It should be emphasized that the new equilibrium causes the post-operative displacement along the 3 axis and does not necessarily (and teleologically) imply either anatomical or functional restoration, as shown in figure 6, where despite 100  $\mu\text{m}$  of post-operative foveal thinning

(fig. 6d), metamorphopsias increased between T3 and T6 while BCVA remained unchanged (fig. 6e).

Interestingly, an average 93  $\mu\text{m}$  loss of foveal thickness, resulted in 148  $\mu\text{m}$  of average *en-face* displacement (table 2), unevenly distributed over the retinal surface and more pronounced at the parafoveal level (165  $\mu\text{m}$ ), compared to the fovea (104  $\mu\text{m}$ ). Chen and coll.<sup>19</sup>, demonstrated that vessels contribute significantly to retinal stiffness and “[...] *vessel size is the only determining factor that governs the anisotropic and inhomogeneous characteristics of the retina*”.

While the functional benefit of ILM peeling performed in our series, compared to ERM stripping alone, remains uncertain<sup>20</sup>, from the mechanical standpoint ILM removal is very likely to trigger significant retinal adjustments since the ILM is a stiff structure<sup>21</sup> whose properties change after peeling and also with staining<sup>22</sup>. A recent meta-analysis reported a significantly thicker post-operative fovea in patients undergoing ILM peeling compared to ERM peeling alone<sup>23</sup>.

The retinal vessels, therefore, represent a true “backbone” responsible for *en-face* displacement that could be exacerbated by ILM removal and whose impact on retinal microcircuitry is unknown. Glial and Muller cells activation progressing from inner to outer retina in response to ERMs, has been previously described<sup>24</sup>, and further modifies the mechanical properties and the response to surgery.

From a purely geometric perspective, 150  $\mu\text{m}$  of *en-face* displacement, exceed the linear dimension of Muller cells and are very likely to determine synaptic disconnection, leading to visual loss. The reason why such macroscopic displacement does not affect vision more profoundly is debatable and may relate to the chronicity of its development and possibly to re-wiring processes<sup>25</sup>, still to be documented. Another reason may lay in the uncertain attribution of *en-face* displacement within the retinal thickness.

The *en-face* displacement we report, in fact, refers to infra-red images where all retinal layers are considered at the same time. Thus, calculated vectors may belong to different layers such as the superficial and deep capillary *plexi*. This notion does not affect the accuracy of displacement itself but cannot localize accurately its depth which implies a much higher and three-dimensional level of complexity, still to be understood.

However, displacement vectors in figures 5 and 6 show elements overtly laying at different depths moving at different rates and directions, unpredictably kinking cells spanning the z-axis: photoreceptors, bipolar, ganglion and Muller cells.

This dynamic scenario may be responsible for the controversial relation between visual function and anatomy<sup>9</sup>: *en-face* displacement along the vertical line of the cross correlated with the change in horizontal metamorphopsia, however the displacement along the horizontal line did not correlate to vertical M-Charts scoring. *En-face* displacement correlated to retinal thinning but not to BCVA improvement, as already reported by Matsumoto<sup>26</sup> in his original paper. This finding may suggest that, apart from thinning, cellular bending also occurring at the level of the z-axis (perpendicular to our *en-face* displacement measures) may play a decisive functional role.

Mieno and Coll.<sup>27</sup> found similar results and even Amsler in 1953<sup>28</sup> reported a greater deformation for horizontal lines than vertical; it is worth mentioning that vertical deformation impacts horizontal line perception and *vice versa*. Allegrini and Coll.<sup>29</sup> measured the displacement of retinal vascular junctions after ERM peeling and found a significant correlation with BCVA changes. As for present study, most changes in both BCVA and *en-face* displacement occurred during the first month post-surgery (figs. 5 and 6), indicating that retinal motion is the primary factor affecting BCVA.

Previous studies suggest that traction induces intraretinal changes mediated by macroglia activation<sup>12</sup> which in turn overexpress glial fibrillary acid proteins in the IRL,

resulting in intraretinal gliosis and the binding between Muller cells and the ILM<sup>30</sup>. Our study also supports these findings since IRL thinning and *en-face* displacements highly correlated ( $p < 0.001$ ) after ERM peeling.

It is conceivable that if gliosis progresses too deep into the retina, it will no longer be able to recover, despite ERM peeling, to the detriment of the nervous elements. Therefore, the ideal surgical timing could be when the retina is still able to move and the intraretinal gliosis hasn't propagated too deep into the retinal layers.

Displacement behaviour as a function of BCVA gain (fig. 4) may support this hypothesis, although the Gaussian distribution of *en-face* displacement may well be a mere feature of pathology itself (as for many distributions). Patients showing the highest and lowest grade of *en-face* displacement equally gained less vision, the former subgroup likely due to their greater initial compromise, and the latter for a "ceiling" effect related to their relatively good pre-op vision. Patients obtaining the highest vision improvement, *vice versa*, belong to the intermediate displacement sub-group, possibly because they started with low vision but less compromised anatomical conditions and/or reversible gliosis. If this held true, the post-operative retinal displacement would be a proof a reversible grade of gliosis and better visual prognosis.

In summary, our study introduced for the first time an accurate and objective measure of *en-face* displacement, demonstrating how deeply the removal of ERMs impacts the entire 3-D retinal architecture. Although the major pitfall is the inability of discern the diverse layers on retinal photos, we believe the incomparably greater number of points examined, offer much greater information, and set the base for further studies.

Finally, we should acknowledge that the concept of surgery as a mechanism of *restitutio ad integrum* is misleading: with all the uncertainties of biomechanical measures, the properties of the entire retina<sup>31</sup>, isolated ILM<sup>32</sup> and ERM<sup>33</sup> are significantly different and

span 2 orders of magnitude; stripping the ERM and ILM from the retinal surface means removing thick and stiff structures adherent to the retina thus macroscopically altering the balance of forces. By no means this can be simplified as “rewinding” the course of disease.

As a final remark, we notice that it will be necessary to expand a detailed assessment of the *en-face* displacement for each retinal layer both before and after surgery to comprehend the functional damage at a cellular level and predict visual outcome and possibly infer the ideal surgical timing.

## Figure Captions

**Fig. 1** – Regions used to analyse the retinal deformation. The yellow lines indicate: **A)** the “central” circular region, 0.5 mm in diameter; **B)** the “perifoveal” annular ring with 0.5 mm and 1.5 mm inner and outer diameters, respectively; **C)** the “parafoveal” annular ring with 1.5 mm and 3 mm inner and outer diameters, respectively. The dashed lines indicate the horizontal and vertical 1 mm wide regions intersecting on the foveola. The background represents in pseudo-colours 2 consecutive images of patient #3 (T0 and T1). The first image is in red while the second image is in green. As a result, red indicates details present only in the first image, green indicates details present only in the second image, while details persisting in both images results yellow. White arrows represent the vector displacement, in magnitude and direction.

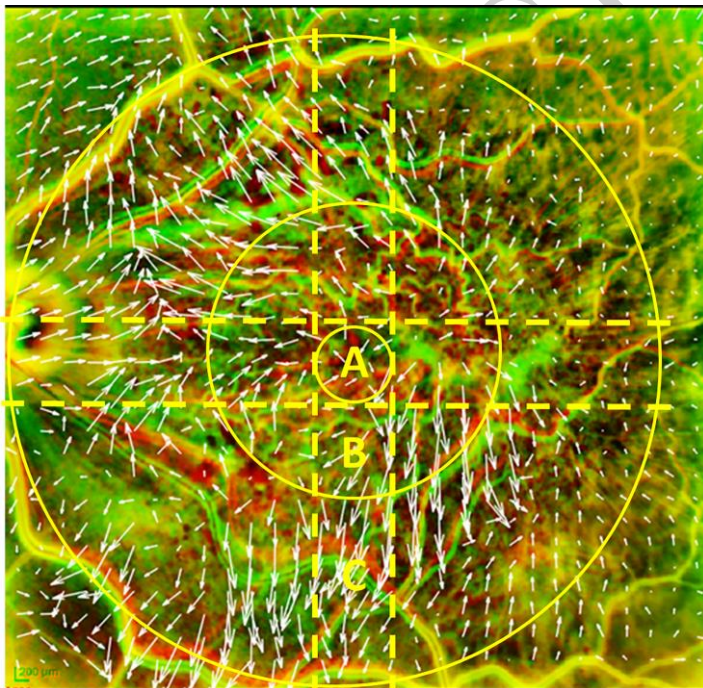




**Fig. 2** – Retinal layer and entire foveal thickness changes across follow-up. Note how most of thickness changes occur in the inner retina.

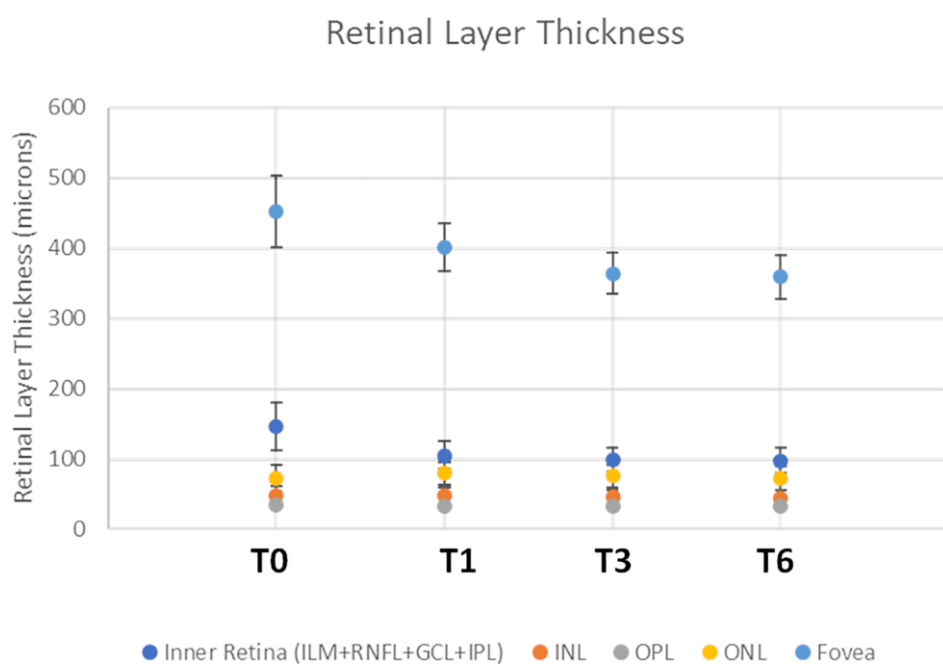


**Fig. 3** – Retinal layer thickness changes (T0-T6) from inner to outer retina and divided by sectors: central foveolar, superior, temporal, inferior and nasal. **a)** Inner Retina (ILM+RNFL+GCL+IPL) including Retinal Nerve Fiber Layer, Ganglion Cell Layer and Inner Plexiform Layer, **b)** Inner Nuclear Layer; **c)** Outer Plexiform Layer; **d)** Outer Nuclear Layer. Concentric circles indicate the foveolar region (radius 0.5 mm), perifoveal (radius 1.5 mm) and parafoveal (radius 3 mm). Numbers indicate thickness changes (in microns), bold numbers indicate a significant reduction in thickness ( $p < 0.05$  for all).

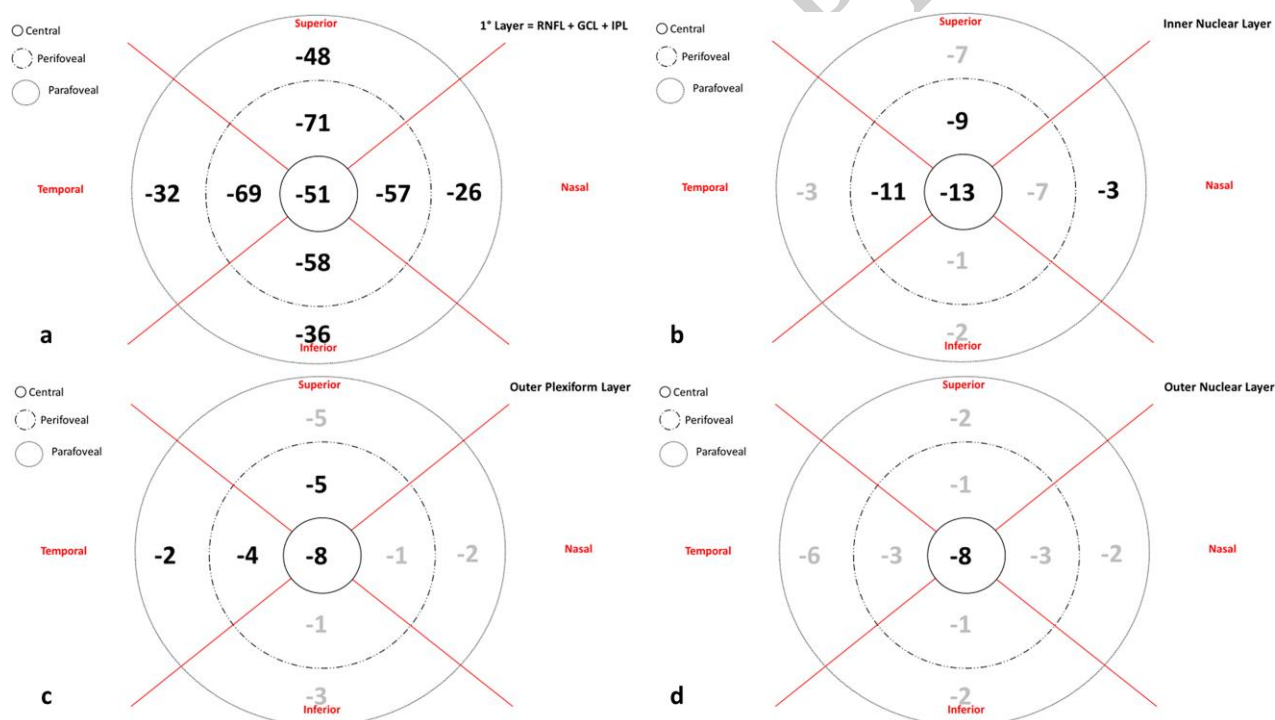


**Fig. 4 –** Distribution of mean *en-face* displacement data as a function of BCVA

increase.

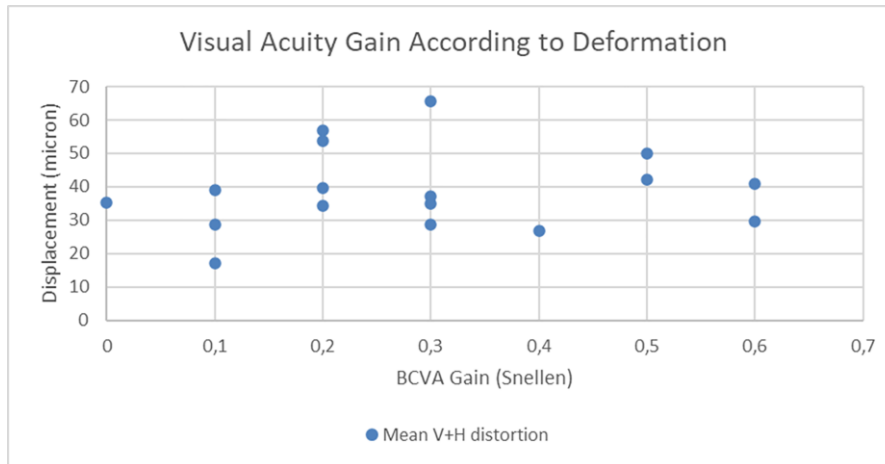


**Fig. 5** – Patient #3. Colour pictures show *en-face* displacements during a) T0-T1; b)

T1-T3; c) T3-T6. Inferior graphs show d) BCVA and OCT foveolar thickness during follow-up; e) Vertical and horizontal metamorphopsia compared to BCVA during follow-up. Most *en-face* displacement occurred during T0-T1 (a) but the fovea kept moving up to T6. Interestingly, despite OCT foveal thinning, BCVA did not improve during T0-T1 (panel d) as metamorphopsias worsened during that time (panel e).

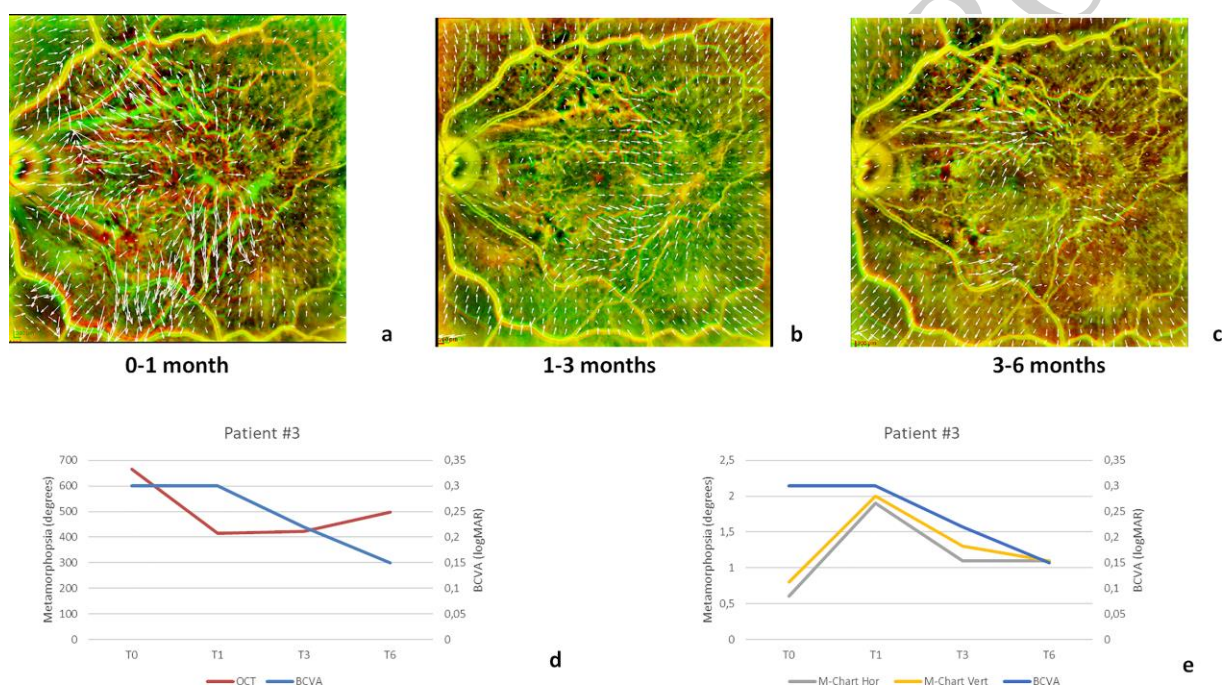
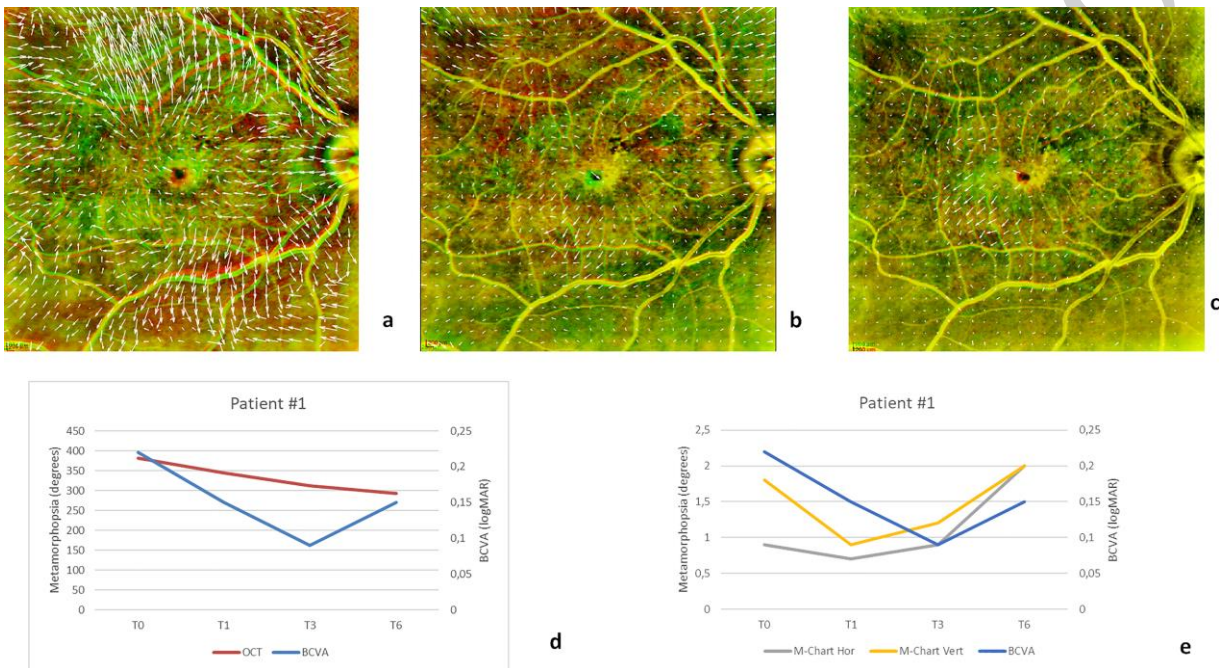


**Fig. 6 – Patient #1.** Colour pictures show *en-face* displacements during a) T0-T1; b)

T1-T3; c) T3-T6. Lower graphs show d) BCVA and OCT foveolar thickness during follow-up; e) Vertical and horizontal metamorphopsia compared to BCVA during follow-up. Note that despite the reduction of foveolar thickness, BCVA increased up to T3 and worsened at T6, while metamorphopsias increased since T1, after initial improvement.



	<b>T0</b>	<b>T1</b>	<b>T3</b>	<b>T6</b>	<b>p</b>
<b>Visual Acuity (Snellen)</b>	0.49 ± 0.13	0.55 ± 0.25	0.62 ± 0.23	0.68 ± 0.12	< 0.05
<b>Horizontal Metamorphopsia (°)</b>	0.91 ± 0.70	0.87 ± 0.48	0.72 ± 0.17	0.78 ± 0.56	n .s.
<b>Vertical Metamorphopsia (°)</b>	1.33 ± 0.70	1.34 ± 0.57	0.84 ± 0.74	0.82 ± 0.69	< 0.05
<b>Microperimetric Sensitivity mean (db)</b>	23.1 ± 4.4	21.2 ± 7.1	22.0 ± 6.5	21.4 ± 7.6	n .s.
<b>Microperimetric Sensitivity 5° (db)</b>	20.7 ± 4.1	20.24 ± 5.6	21.1 ± 4.7	20.9 ± 5.8	n .s.
<b>Microperimetric Sensitivity 10° (db)</b>	22.9 ± 4.4	19.7 ± 8.3	22.1 ± 5.7	21.8 ± 6.7	n .s.

**Table 1** – Best Corrected Visual Acuity, metamorphopsia and microperimetric sensitivity throughout follow-up

	0-1 months	1-3 months	3-6 months	0-6 months
<b>Central Foveal Thickness Change</b>	-52.4 ± 136.8	-38.3 ± 46	-2.58 ± 43.3	-93.3 ± 124.1
<b>Overall Displacement (6x6 mm field)</b>	83.5 ± 30.2	36.2 ± 14.4	39.1 ± 22.7	148.8 ± 24.1
<b>Central Circle (0.5mm radius)</b>	46.4 ± 28.4	22.9 ± 18.3	30.5 ± 19.0	104.7 ± 25.3
<b>Perifoveal Crown (1.5mm radius)</b>	62.3 ± 37.5	67.8 ± 38.2	29.5 ± 16.4	159.6 ± 29.1
<b>Parafoveal Crown (3mm radius)</b>	82.4 ± 52.7	50.0 ± 28.1	33.2 ± 18.1	165.6 ± 31.4

**Table 2** – En-Face Displacement in microns, throughout follow-up of central 6x6mm field and concentric EDTRS areas.

## References

- <sup>1</sup> Fung AT, Galvin J, Tran T. Epiretinal membrane: A review. *Clin Exp Ophthalmol*. 2021 Apr;49(3):289-308. doi: 10.1111/ceo.13914. Epub 2021 Mar 24. PMID: 33656784.
- <sup>2</sup> Brinkmann A, Unterlauff JD, Barth T, et al. Foveal configurations with disappearance of the foveal pit in eyes with macular pucker: Presumed role of Müller cells in the formation of foveal herniation. *Exp Eye Res*. 2021 Jun;207:108604. doi: 10.1016/j.exer.2021.108604. Epub 2021 Apr 27. PMID: 33930399.
- <sup>3</sup> Simunovic, Matthew P. MB BChir, PhD, FRANZCO\*,†,‡. METAMORPHOPSIA AND ITS QUANTIFICATION. *Retina* 35(7):p 1285-1291, July 2015. | DOI: 10.1097/IAE.0000000000000581
- <sup>4</sup> Xu K, Gupta V, Bae S, Sharma S. Metamorphopsia and vision-related quality of life among patients with age-related macular degeneration. *Can J Ophthalmol*. 2018 Apr;53(2):168-172. doi: 10.1016/j.jcjo.2017.08.006. Epub 2017 Oct 25. PMID: 29631830.
- <sup>5</sup> Ichikawa Y, Imamura Y, Ishida M. Inner Nuclear Layer Thickness, a Biomarker of Metamorphopsia in Epiretinal Membrane, Correlates With Tangential Retinal Displacement. *Am J Ophthalmol*. 2018 Sep;193:20-27. doi: 10.1016/j.ajo.2018.06.001. Epub 2018 Jun 8. PMID: 29890161.
- <sup>6</sup> Sakai D, Takagi S, Hirami Y, et al. Correlation between tangential distortion of the outer retinal layer and metamorphopsia in patients with epiretinal membrane. *Graefes Arch Clin Exp Ophthalmol*. 2021 Jul;259(7):1751-1758. doi: 10.1007/s00417-021-05077-4. Epub 2021 Jan 16. PMID: 33452907; PMCID: PMC8277649.
- <sup>7</sup> Nakano E, Ota T, Jingami Y, et al. Correlation between metamorphopsia and disorganization of the retinal inner layers in eyes with diabetic macular edema. *Graefes Arch Clin Exp Ophthalmol*. 2019 Sep;257(9):1873-1878. doi: 10.1007/s00417-019-04393-0. Epub 2019 Jun 22. PMID: 31227899.
- <sup>8</sup> Chan EW, Eldeeb M, Sun V, et al. Disorganization of Retinal Inner Layers and Ellipsoid Zone Disruption Predict Visual Outcomes in Central Retinal Vein Occlusion. *Ophthalmol Retina*. 2019 Jan;3(1):83-92. doi: 10.1016/j.oret.2018.07.008. Epub 2018 Oct 19. PMID: 30929820.
- <sup>9</sup> Chang S, Gregory-Roberts EM, Park S, et al. Double peeling during vitrectomy for macular pucker: the Charles L. Schepens Lecture. *JAMA Ophthalmol*. 2013 Apr;131(4):525-30. doi: 10.1001/jamaophthalmol.2013.2176. PMID: 23579603.
- <sup>10</sup> Zeyer JC, Parker P, Dajani O, MacCumber MW. Preoperative Domed Macular Contour Correlates With Postoperative Visual Gain After Vitrectomy For Symptomatic Epiretinal Membrane. *Retina*. 2021 Mar 1;41(3):505-509. doi: 10.1097/IAE.0000000000002869. PMID: 32568987.
- <sup>11</sup> Govetto A, Lalane RA 3rd, Sarraf D, et al. Insights Into Epiretinal Membranes: Presence of Ectopic Inner Foveal Layers and a New Optical Coherence Tomography Staging Scheme. *Am J Ophthalmol*. 2017 Mar;175:99-113. doi: 10.1016/j.ajo.2016.12.006. Epub 2016 Dec 18. PMID: 27993592.
- <sup>12</sup> Govetto A, Lalane RA 3rd, Sarraf D, et al. Insights Into Epiretinal Membranes: Presence of Ectopic Inner Foveal Layers and a New Optical Coherence Tomography Staging Scheme. *Am J Ophthalmol*. 2017 Mar;175:99-113. doi: 10.1016/j.ajo.2016.12.006. Epub 2016 Dec 18. PMID: 27993592.
- <sup>13</sup> Arimura E, Matsumoto C, Nomoto H, et al. Correlations between M-CHARTS and PHP findings and subjective perception of metamorphopsia in patients with macular diseases. *Invest Ophthalmol Vis Sci*. 2011 Jan 5;52(1):128-35. doi: 10.1167/iovs.09-3535. PMID: 20739469.
- <sup>14</sup> Parravano M, De Geronimo D, Scarinci F, et al. Progression of Diabetic Microaneurysms According to the Internal Reflectivity on Structural Optical Coherence Tomography and Visibility on Optical Coherence Tomography Angiography. *Am J Ophthalmol*. 2019 Feb;198:8-16. doi: 10.1016/j.ajo.2018.09.031. Epub 2018 Oct 9. PMID: 30308201.
- <sup>15</sup> Cacciamani A, Cosimi P, Di Nicola M, et al. Correlation Between Outer Retinal Thickening And Retinal Function Impairment In Patients With Idiopathic Epiretinal Membranes. *Retina*. 2019 Feb;39(2):331-338. doi: 10.1097/IAE.0000000000001971. PMID: 29190229.
- <sup>16</sup> Farneback, G. "Two-Frame Motion Estimation Based on Polynomial Expansion." In *Proceedings of the 13th Scandinavian Conference on Image Analysis*, 363 - 370. Halmstad, Sweden: SCIA, 2003.
- <sup>17</sup> Nguyen JH, Yee KM, Sadun AA, Sebag J. Quantifying Visual Dysfunction and the Response to Surgery in Macular Pucker. *Ophthalmology*. 2016 Jul;123(7):1500-10. doi: 10.1016/j.ophtha.2016.03.022. Epub 2016 Apr 27. PMID: 27129901.
- <sup>18</sup> Chua PY, Sandinha MT, Steel DH. Idiopathic epiretinal membrane: progression and timing of surgery. *Eye (Lond)*. 2022 Mar;36(3):495-503. doi: 10.1038/s41433-021-01681-0. Epub 2021 Jul 21. PMID: 34290446; PMCID: PMC9074182.



- <sup>19</sup> Chen K, Weiland JD. Anisotropic and inhomogeneous mechanical characteristics of the retina. *J Biomech.* 2010 May 7;43(7):1417-21. doi: 10.1016/j.jbiomech.2009.09.056. Epub 2010 Feb 8. PMID: 20116062.
- <sup>20</sup> Fang XL, Tong Y, Zhou YL, et al. Internal limiting membrane peeling or not: a systematic review and meta-analysis of idiopathic macular pucker surgery. *Br J Ophthalmol.* 2017;101:1535-1541. doi: 10.1136/bjophthalmol-2016-309768. Epub 2017 Mar 17. PMID: 28314834.
- <sup>21</sup> Vielmuth F, Schumann RG, Spindler V et al. Biomechanical Properties of the Internal Limiting Membrane after Intravitreal Ocriplasmin Treatment. *Ophthalmologica.* 2016;235:233-40. doi: 10.1159/000444508. Epub 2016 Apr 28. PMID: 27120551.
- <sup>22</sup> Haritoglou C, Mauell S, Benoit M et al. Vital dyes increase the rigidity of the internal limiting membrane. *Eye (Lond).* 2013;27:1308-15. doi: 10.1038/eye.2013.178. Epub 2013 Aug 16. PMID: 23949493; PMCID: PMC3831134.
- <sup>23</sup> Sun Y, Zhou R, Zhang B. With Or Without Internal Limiting Membrane Peeling For Idiopathic Epiretinal Membrane: A Meta-Analysis of Randomized Controlled Trials. *Retina.* 2021 Aug 1;41(8):1644-1651. doi: 10.1097/IAE.0000000000003076. PMID: 33394964.
- <sup>24</sup> Bringmann A, Unterlauff JD, Barth T, et al. Müller cells and astrocytes in tractional macular disorders. *Prog Retin Eye Res.* 2022 Jan;86:100977. doi: 10.1016/j.preteyeres.2021.100977. Epub 2021 Jun 5. PMID: 34102317.
- <sup>25</sup> Gao H, Huang X, He J et al. The roles of microglia in neural remodeling during retinal degeneration. *Histol Histopathol.* 2022 Jan;37(1):1-10. doi: 10.14670/HH-18-384. Epub 2021 Oct 25. PMID: 34693982.
- <sup>26</sup> Matsumoto C, Arimura E, Okuyama S, et al. Quantification of metamorphopsia in patients with epiretinal membranes. *Invest Ophthalmol Vis Sci.* 2003 Sep;44(9):4012-6. doi: 10.1167/iovs.03-0117. PMID: 12939323.
- <sup>27</sup> Mieno H, Kojima K, Yoneda K, et al. Evaluation of pre- and post-surgery reading ability in patients with epiretinal membrane: a prospective observational study. *BMC Ophthalmol.* 2020 Mar 10;20(1):95. doi: 10.1186/s12886-020-01364-6. PMID: 32156267; PMCID: PMC7063750.
- <sup>28</sup> Amsler M. Earliest symptoms of diseases of the macula. *Br J Ophthalmol.* 1953 Sep;37(9):521-37. doi: 10.1136/bjo.37.9.521. PMID: 13081950; PMCID: PMC1324189.
- <sup>29</sup> Allegrini D, Montesano G, Marconi S et al. A novel quantitative analysis method for idiopathic epiretinal membrane. *PLoS One.* 2021 Mar 17;16(3):e0247192. doi: 10.1371/journal.pone.0247192.
- <sup>30</sup> Romano MR, Ilardi G, Ferrara M, et al. Intraretinal changes in idiopathic versus diabetic epiretinal membranes after macular peeling. *PLoS One.* 2018; 13(5):1-12.
- <sup>31</sup> Ferrara M, Lugano G, Sandinha MT et al. Biomechanical properties of retina and choroid: a comprehensive review of techniques and translational relevance. *Eye (Lond).* 2021;35:1818-1832. doi: 10.1038/s41433-021-01437-w. Epub 2021 Mar 1. PMID: 33649576; PMCID: PMC8225810.
- <sup>32</sup> Vielmuth F, Schumann RG, Spindler V et al. Biomechanical Properties of the Internal Limiting Membrane after Intravitreal Ocriplasmin Treatment. *Ophthalmologica.* 2016;235(4):233-40. doi: 10.1159/000444508. Epub 2016 Apr 28. PMID: 27120551.
- <sup>33</sup> Ciasca G, Pagliei V, Minelli E et al. Nanomechanical mapping helps explain differences in outcomes of eye microsurgery: A comparative study of macular pathologies. *PLoS One.* 2019 Aug 7;14(8):e0220571. doi: 10.1371/journal.pone.0220571. PMID: 31390353; PMCID: PMC6685617.